



Pergamon

Bioorganic & Medicinal Chemistry Letters 9 (1999) 1317–1322

BIOORGANIC &
MEDICINAL CHEMISTRY
LETTERS

Optimisation of the P2 Pharmacophore in a Series of Thrombin Inhibitors : Ion-dipole Interactions with Lysine 60G

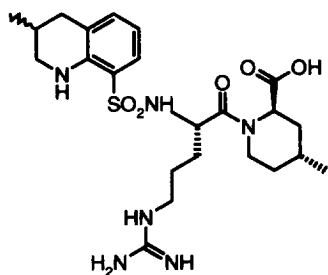
John Ambler, Lyndon Brown, Xiao-Ling Cockcroft, Markus Grütter, Judy Hayler, Diana Janus, Darryl Jones, Peter Kane, Keith Menear*, John Priestle, Garrick Smith, Mark Talbot, Clive V Walker & Bernard Wathey
Novartis Horsham Research Center, Wimblehurst Road, Horsham, West Sussex RH12 4AB

Received 25 January 1999; accepted 1 April 1999

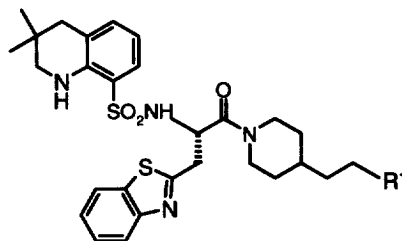
Abstract : The optimisation of the P2 pharmacophore in a series of thrombin inhibitors is described. The interaction of a number of piperidine P2 functionalities with lysine 60G of thrombin is explored with reference to the crystal structure of inhibitor enzyme complexes. A primary ion-dipole interaction between the terminal P2 side chain group and lysine 60G is evoked to explain the SAR in this series. © 1999 Elsevier Science Ltd. All rights reserved.

Thrombin has become a principal target in the search for new anticoagulants due to its pre-eminence as a mediator in blood coagulation. It is proposed that inhibitors of thrombin will find utility in the treatment and prevention of cardiovascular disorders such as deep vein thrombosis, myocardial infarction and stroke.^{1,2}

From the archetypal reversible thrombin inhibitor MD805³ **1** our efforts have lead to the discovery of highly potent competitive thrombin inhibitors represented by the core structure **2** bearing a neutral benzthiazolylalanine in P1 and a dimethyltetrahydroquinoline pharmacophore in P3.^{4,5} Herein we describe the optimisation of the P2 pharmacophore in this series of compounds, specifically the effect on potency of modulating the terminal piperidine side chain functionality.



1



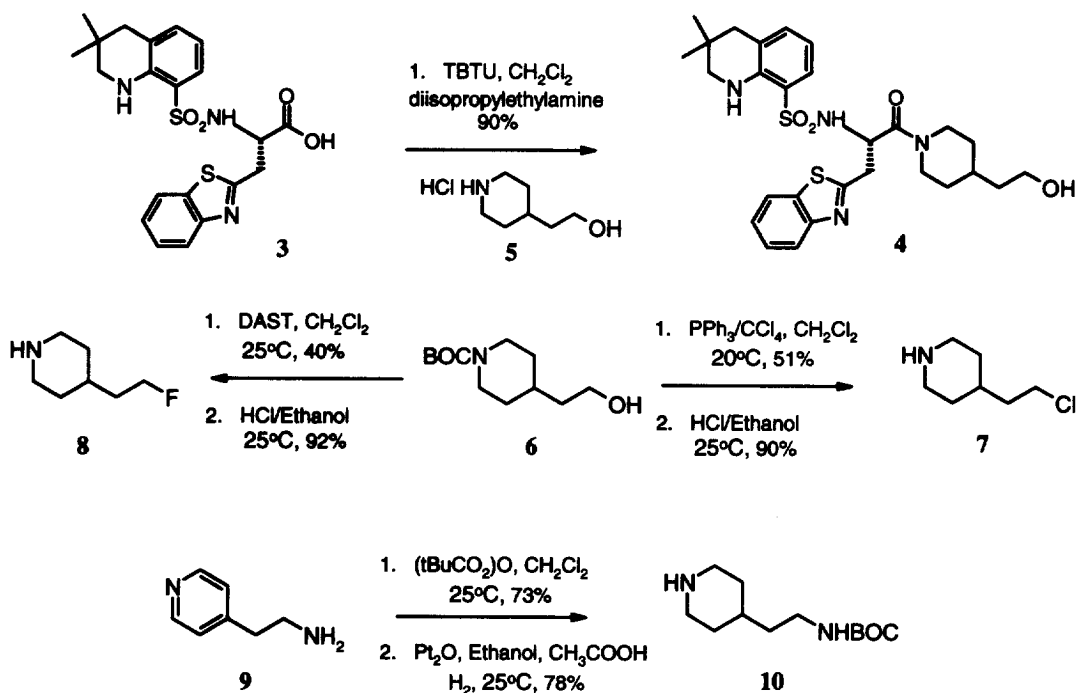
2

Synthetic access to the compounds detailed in this work is exemplified by the synthesis of **4** from **3** (Scheme 1). Standard peptide coupling conditions using 2-(1H-benzotriazol-1-yl)-1,1,3,3-tetramethyluronium tetrafluoroborate (TBTU) on acid **3** provided **4** on treatment with 2-piperidin-4-yl-ethanol **5**. The 4-(2-chloroethyl)-piperidine **7** was prepared by direct chlorination from the BOC protected hydroxyethylpiperidine **6** under standard conditions followed by acidic deprotection. The BOC-hydroxyethylpiperidine **6** also served as a starting material for the synthesis of **8** which was generated on treatment of **6** with diethylaminosulfur trifluoride (DAST).

e mail keith.menear@pharma.novartis.com Fax +44(0)1403 323307

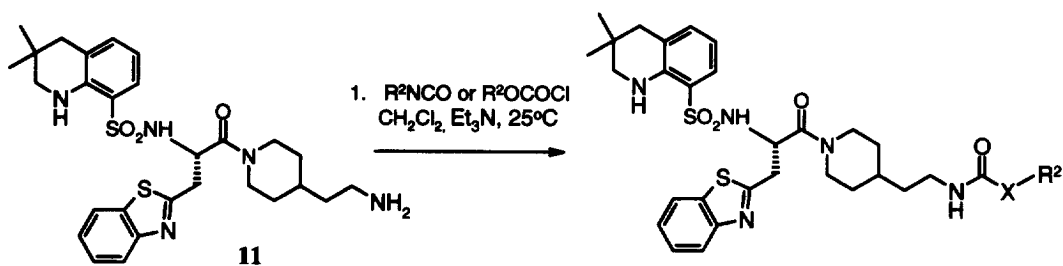
0960-894X/99/\$ - see front matter © 1999 Elsevier Science Ltd. All rights reserved.

PII: S0960-894X(99)00172-9



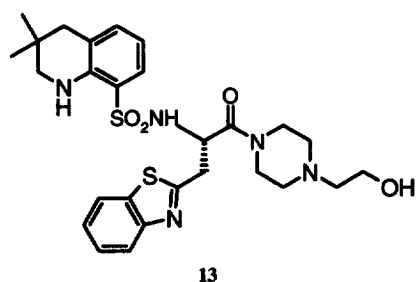
Scheme 1

BOC protection of 2-(2-aminoethyl)pyridine **9** followed by reductive hydrogenation gave **10**, which on coupling to acid **3** and acidic deprotection provided **11**. Amine **11** subsequently gave entry into compounds **18–22**, **24**, **25** and **26** on reaction with the respective acid chlorides or isocyanates according to the general sequence in Scheme 2.

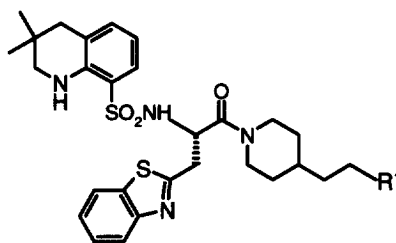


Scheme 2

The *in vitro* potency of compounds was evaluated as the inhibition constant (K_i) determined against human thrombin. Analysis of the X-ray crystal structure⁶ of thrombin complexed with analog **13** (K_i 0.35 μM), a related piperazine derivative (Figure 1), allowed us to extrapolate structural information on the bound conformation of **13** to the piperidine series under discussion.

**Figure 1**

Notable from analysis of the crystal structure of **13** bound to thrombin is the favorable interaction of the P2 hydroxyl oxygen with lysine 60G (Lys 60G) of thrombin. Despite the fact that the piperazine in P2 will deliver the side chain in a slightly different orientation, it was reasoned that the primary P2 interaction to Lys 60G would be maintained in the equivalent piperidine compounds. To capitalise on this feature derivatives **12**, **14** and **15** were synthesised (Table 1). A potency order is observed in the sequence F>OH>Cl>H, the activity trend following the atomic electronegativity (χ) values of the corresponding side chain functionality.

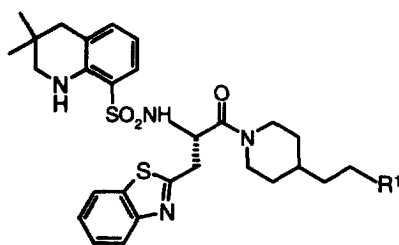
Table 1

Compound	R ¹	Ki (μM)	χ
15	F	0.026	4.0
4	OH	0.079	3.5
14	Cl	0.093	2.8
12	H	0.240	2.2

It is unlikely that the increase in potency on going from the hydroxyl in **4** to the fluorine in **15** can be attributed to an increased capacity for hydrogen bonding to Lys 60G. The F \cdots H hydrogen bond is weak (2–3.2 kcal mol⁻¹ *vis a vis* an O \cdots H hydrogen bond between 5–10 kcal mol⁻¹) and there is little experimental evidence to evoke strong F \cdots H bonds⁷. It is more reasonable to assume an ion-dipole interaction between the fluorine and

the surface exposed Lys 60G, since at physiological pH the ϵ -amino group of the lysine will be protonated (lysine pKa 10.25). This assumption is supported by the enhancement in potency with increased χ values across the series described in Table 1. Since the carbonyl oxygen of urea and urethane groups are also known to have high δ^- values⁸, a second series of compounds was synthesised based on these modalities (Table 2).

Table 2



Compound	R ¹	Ki (μM)	Compound	R ¹	Ki (μM)
16		0.038	22		1.00
17		0.056	11	NH ₂	1.18
18		0.052	23	NMe ₂	38.32
19		0.024	24	COOH	7.83
20		0.065	25		0.654
21		0.182	26		0.119

As predicted both the urethane and urea derivatives give rise to highly potent inhibitors as witnessed by the Ki values for compounds **17** and **19**. Although the reason is unclear, larger and more lipophilic groups were tolerated in the carbamate series in comparison to the urea derivatives where potency drops with increasing length of the side chain as exemplified in the series **19**, **20** and **21**. Also consistent with the SAR is the observation that the amino and dimethylamino derivatives **11** and **23** are weak inhibitors, presumably due to cationic repulsion between the protonated side chain residues and Lys 60G. Other examples in this series are the amide **25** and sulfamide **26**. Intriguingly the carboxylic acid **24** demonstrates low potency where one would expect a favorable salt bridge to be formed between inhibitor and enzyme. This result may be rationalised by the observation that a number of acidic P2 pharmacophores proved inactive and access of acid residues into this occluded lipophilic pocket may be problematic.

To further characterise this series of compounds the X-ray crystal structure⁶ of urethane **18** bound to thrombin was determined (Figure 2).

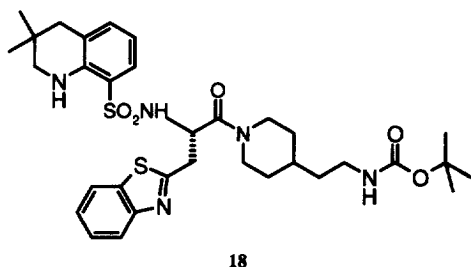


Figure 2

From the crystal structure it is apparent that the urethane carbonyl oxygen in **18** forms a favorable ion-dipole interaction with a distance to Lys 60G of 2.44 Å. This compares with a distance of 2.7 Å for the oxygen-Lys distance for **13**. What is also noteworthy is the considerable shift in the amino acid residues of the specificity loop of thrombin bound to **18** respective to **13** (Figure 3). On comparison of the two crystal structures it is clear that Lys 60G, tryptophan 60B and glutamic acid E192 move 2.3, 1.1 and 1.3 Å respectively, to accommodate the larger side chain in **18**.

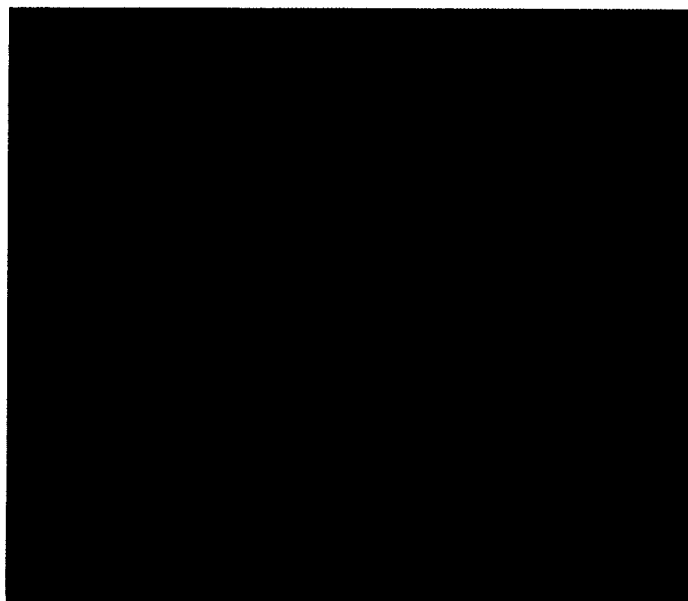


Figure 3

The enhancement of potency in the urethane series may also be attributed to the replacement of the water molecule noted in the crystal structure of **13** by the substituted sp^3 oxygen atom of the urethane in **18**. This supposition is supported by amide **25**, having a methyl group at the corresponding position, which displays only relatively weak activity. In conclusion, we have illustrated that by examination of the binding mode of two of our thrombin inhibitors co-crystallised with the enzyme further optimisation of the P2 pharmacophore is possible. By refinement of the ion-dipole interaction between the terminal P2 piperidine side chain and Lys 60G high potency thrombin inhibitors have been achieved. Elaboration of these compounds to provide potent selective and bioavailable thrombin inhibitors will be the subject of subsequent publications.

References and Notes

1. Turpie, Alexander G. G.; Weitz, Jeffrey I.; Hirsh, Jack. *Thromb. Haemostasis* (1995), 74(1), 565-571.
2. Fenton, J. W., II; Ofosu, F. A.; Moon, D. G.; Maraganore, J. M. *Blood Coagulation Fibrinolysis* (1991), 2(1), 69-75.
3. Kikumoto, Ryoji; Tamao, Yoshikuni; Ohkubo, Kazuo; Tezuka, Tohru; Tonomura, Shinji; Okamoto, Shosuke; Hijikata, Akiko. *J. Med. Chem.* (1980), 23(12), 1293-1299.
4. For convenience pharmacophores residing in the S9 pocket, also known as the distal or aryl pocket, of thrombin are referred to as P3.
5. Studies relating to the discovery of **2** is in press. Mark C. Allen, John Ambler, Derek E. Brundish, Alice Bull, Vera Donovan, Joseph D. Fullerton, Sheila M. Garman, Judy F. Hayler, Geoffrey Howarth, William Hoyle, Diana Janus, Peter D Kane*, Mark McDonnell, Garrick P. Smith, Mark D. Talbot, Robert Wakeford, Clive V. Walker. *J. Med. Chem.* in press
6. The C-terminal fragment of hirudin (residues 54-65, sulfated Tyr-63), a natural inhibitor of thrombin from the European medicinal leech *Hirudo medicinalis*, was used to prepare well-diffracting crystals of thrombin reproducibly. A 1:1 molar ratio of thrombin:hirudin was set up against buffered sodium chloride in hanging drop experiments. Large, well-formed crystals grew within two weeks. Compounds **13** and **18** were soaked into the pre-formed crystals of the thrombin-hirudin fragment complex by adding a small amount of substance directly to a drop containing a thrombin crystal. Diffraction data were collected on a FAST area detector (Nonius) with a rotating anode generator providing graphite-monochromated CuK_{α} X-radiation. Crystals of the inhibitor-thrombin complexes were shown to belong to space group C2 with unit cell parameters $a=71.9\text{\AA}$, $b=72.1\text{\AA}$, $c=72.9\text{\AA}$, $\beta=101.0^\circ$ (with compound **13**) and $a=71.5\text{\AA}$, $b=72.2\text{\AA}$, $c=73.0\text{\AA}$, $\beta=101.0^\circ$ (with compound **18**), with one molecule of the complex (thrombin, C-terminal fragment of hirudin and inhibitor) in the asymmetric unit. Diffraction data to 2.0\AA resolution could be collected for the complex with compound **13**, while the crystal complexed with compound **18** diffracted to only 2.5\AA . The structure of the complex with compound **13** was solved using molecular replacement employing thrombin alone as the trial structure. The structure was partially refined before trying to build in the inhibitor in order to improve the quality of the electron density for the inhibitor. An Fo-Fc difference Fourier showed very clear density for the inhibitor in the active site and the chemical structure of compound **13**. Further refinement, including the addition of solvent molecules, was carried out until no improvement in the structure could be realised. The structure of the complex with compound **18** was solved by using the structure of the complex with compound **13**, after removing the inhibitor and solvent molecules, since the crystal forms are isomorphous. Again there was electron density in the active site for the inhibitor which fit the chemical structure of compound **18**. Although the quality of the density was inferior to that for the previous structure, the inhibitor could be unambiguously fitted into the electron density and refined. The solid surface of thrombin is generated by Quanta 79.
7. Howard, Judith A. K.; Hoy, Vanessa J.; O'Hagan, David; Smith, Garry T. *Tetrahedron* (1996), 52(38), 12613-12622.
8. Abraham, Michael H.; Duce, Philip P.; Prior, David V.; Barratt, Derek G.; Morris, Jeffrey J.; Taylor, Peter J. *J. Chem. Soc., Perkin Trans. 2* (1989), 10, 1355-75.